100-kHz shot-to-shot broadband data acquisition for high-repetition-rate pump–probe spectroscopy

Florian Kanal,[1] **Sabine Keiber,**[1,2] **Reiner Eck,**[1] **and Tobias Brixner**[1,*]

[1]*Institut für Physikalische und Theoretische Chemie, Universität Würzburg, Am Hubland, 97074 Würzburg, Germany*

[2]*Current address: Max-Planck-Institut für Quantenoptik, Hans-Kopfermann-Str. 1, 85748 Garching, Germany*

[*]*brixner@phys-chemie.uni-wuerzburg.de*

Abstract: Shot-to-shot broadband detection is common in ultrafast pump–probe spectroscopy. Taking advantage of the intensity correlation of subsequent laser pulses improves the signal-to-noise ratio. Finite data read-out times of CCD chips in the employed spectrometer and the maximum available speed of mechanical pump-beam choppers typically limit this approach to lasers with repetition rates of a few kHz. For high-repetition ($\geq$ 100 kHz) systems, one typically averages over a larger number of laser shots leading to inferior signal-to-noise ratios or longer measurement times. Here we demonstrate broadband shot-to-shot detection in transient absorption spectroscopy with a 100-kHz femtosecond laser system. This is made possible using a home-built high-speed chopper with external laser synchronization and a fast CCD line camera. Shot-to-shot detection can reduce the data acquisition time by two orders of magnitude compared to few-kHz lasers while keeping the same signal-to-noise ratio.

OCIS codes: (040.1490) Cameras; (040.1520) CCD, charge-coupled device; (230.4110) Modulators; (300.6500) Spectroscopy, time-resolved; (300.6530) Spectroscopy, ultrafast; (320.7100) Ultrafast measurements.

References and links

1. A. H. Zewail, "Femtochemistry: atomic-scale dynamics of the chemical bond," J. Phys. Chem. A **104**, 5660–5694 (2000).
2. T. Polack, "Spectroscopie infrarouge impulsionnelle appliquée au transfert de ligands dans les hémoprotéines," Ph.D. thesis, École Polytechnique, Paris (2003).
3. T. Polack, J. P. Ogilvie, S. Franzen, M. H. Vos, M. Joffre, J.-L. Martin, and A. Alexandrou, "CO vibration as a probe of ligand dissociation and transfer in myoglobin," Phys. Rev. Lett. **93**, 018102 (2004).
4. G. Auböck, C. Consani, R. Monni, A. Cannizzo, F. v. Mourik, and M. Chergui, "Femtosecond pump/supercontinuum-probe setup with 20 kHz repetition rate," Rev. Sci. Instrum. **83**, 093105 (2012).
5. P. Tournois, "Acousto-optic programmable dispersive filter for adaptive compensation of group delay time dispersion in laser systems," Opt. Commun. **140**, 245–249 (1997).
6. J. Buback, M. Kullmann, F. Langhojer, P. Nuernberger, R. Schmidt, F. Würthner, and T. Brixner, "Ultrafast bidirectional photoswitching of a spiropyran," J. Am. Chem. Soc. **132**, 16510–16519 (2010).
7. U. Megerle, I. Pugliesi, C. Schriever, C. Sailer, and E. Riedle, "Sub-50 fs broadband absorption spectroscopy with tunable excitation: Putting the analysis of ultrafast molecular dynamics on solid ground," Appl. Phys. B **96**, 215–231 (2009).
8. S. D. McClure, D. B. Turner, P. C. Arpin, T. Mirkovic, and G. D. Scholes, "Coherent oscillations in the PC577 cryptophyte antenna occur in the excited electronic state," J. Phys. Chem. B **118**, 1296–1308 (2014).

#209006 - $15.00 USD Received 26 Mar 2014; revised 9 May 2014; accepted 19 May 2014; published 3 Jul 2014

9. J. Piel, E. Riedle, L. Gundlach, R. Ernstorfer, and R. Eichberger, "Sub-20 fs visible pulses with 750 nJ energy from a 100 kHz noncollinear optical parametric amplifier," Opt. Lett. **31**, 1289–1291 (2006).
10. A. Yabushita, Y.-H. Lee, and T. Kobayashi, "Development of a multiplex fast-scan system for ultrafast time-resolved spectroscopy," Rev. Sci. Instrum. **81**, 063110 (2010).
11. M. J. Feldstein, P. Vöhringer, and N. F. Scherer, "Rapid-scan pump-probe spectroscopy with high time and wave-number resolution: optical-Kerr-effect measurements of neat liquids," J. Opt. Soc. Am. B **12**, 1500–1510 (1995).
12. K. F. Lee, A. Bonvalet, P. Nuernberger, and M. Joffre, "Unobtrusive interferometer tracking by path length oscillation for multidimensional spectroscopy," Opt. Express **17**, 12379–12384 (2009).
13. Y. H. Meyer, M. Pittman, and P. Plaza, "Transient absorption of symmetrical carbocyanines," J. Photochem. Photobiol. A **114**, 1–21 (1998).
14. D. Wang, H. Jiang, H. Yang, C. Liu, Q. Gong, J. Xiang, and G. Xu, "Investigation on photoexcited dynamics of IR-140 dye in ethanol by femtosecond supercontinuum-probing technique," J. Opt. A: Pure Appl. Opt. **4**, 155–159 (2002).
15. D. Wang, H. Jiang, S. Wu, H. Yang, Q. Gong, J. Xiang, and G. Xu, "An investigation of solvent effects on the optical properties of dye IR-140 using the pump supercontinuum-probing technique," J. Opt. A: Pure Appl. Opt. **5**, 515–519 (2003).
16. M. Bradler, P. Baum, and E. Riedle, "Femtosecond continuum generation in bulk laser host materials with sub-μJ pump pulses," Appl. Phys. B **97**, 561–574 (2009).
17. I. H. M. van Stokkum, D. S. Larsen, and R. van Grondelle, "Global and target analysis of time-resolved spectra," Biochim. Biophys. Acta, Bioenerg. **1657**, 82–104 (2004).
18. J. J. Snellenburg, S. P. Laptenok, R. Seger, K. M. Mullen, and I. H. M. van Stokkum, "Glotaran: a Java-based Graphical User Interface for the R-package TIMP," Journal of Statistical Software **49**, 1–22 (2012).
19. K. M. Mullen and I. H. M. van Stokkum, "TIMP: an R package for modeling multi-way spectroscopic measurements," J. Stat. Softw. **18**, 1–46 (2007).
20. C. Schriever, S. Lochbrunner, E. Riedle, and D. J. Nesbitt, "Ultrasensitive ultraviolet-visible 20 fs absorption spectroscopy of low vapor pressure molecules in the gas phase," Rev. Sci. Instrum. **79**, 013107 (2008).
21. D. Polli, L. Lüer, and G. Cerullo, "High-time-resolution pump-probe system with broadband detection for the study of time-domain vibrational dynamics," Rev. Sci. Instrum. **78**, 103108 (2007).
22. D. Linde, "Characterization of the noise in continuously operating mode-locked lasers," Appl. Phys. B **39**, 201–217 (1986).

1. Introduction

Ultrafast optical time-resolved pump–probe spectroscopy is a versatile tool to study dynamics of light-induced molecular processes [1]. Among them are energy and charge transfer, conformational changes and primary reaction steps of photochemical reactions which occur on a subpicosecond to nanosecond timescale. In transient absorption spectroscopy, an ultrafast pump pulse excites a subensemble of a molecular sample and a second laser pulse probes the absorption as a function of wavelength λ and delay time τ. The absorbance a of each probe pulse is defined by the intensity of the incident (I_0) and transmitted light (I) in the Beer–Lambert law,

$$a = \lg \frac{I_0}{I}, \tag{1}$$

via the decadic logarithm, lg. Experimentally, one is interested in the change in absorbance Δa induced by the pump pulse defined as the difference between the absorbance of the pumped (a_p) and the unpumped sample (a_u):

$$\Delta a = a_\mathrm{p} - a_\mathrm{u} = \lg \frac{I_0}{I_\mathrm{p}} - \lg \frac{I_0'}{I_\mathrm{u}}. \tag{2}$$

Typically, however, one does not measure the incident probe intensities I_0 and I_0' for the times when the pump pulse is present and absent, respectively. Rather one calculates the absorbance change in an approximate but simplified version from

$$\Delta a = \lg \frac{I_\mathrm{u}}{I_\mathrm{p}}. \tag{3}$$

#209006 - $15.00 USD Received 26 Mar 2014; revised 9 May 2014; accepted 19 May 2014; published 3 Jul 2014

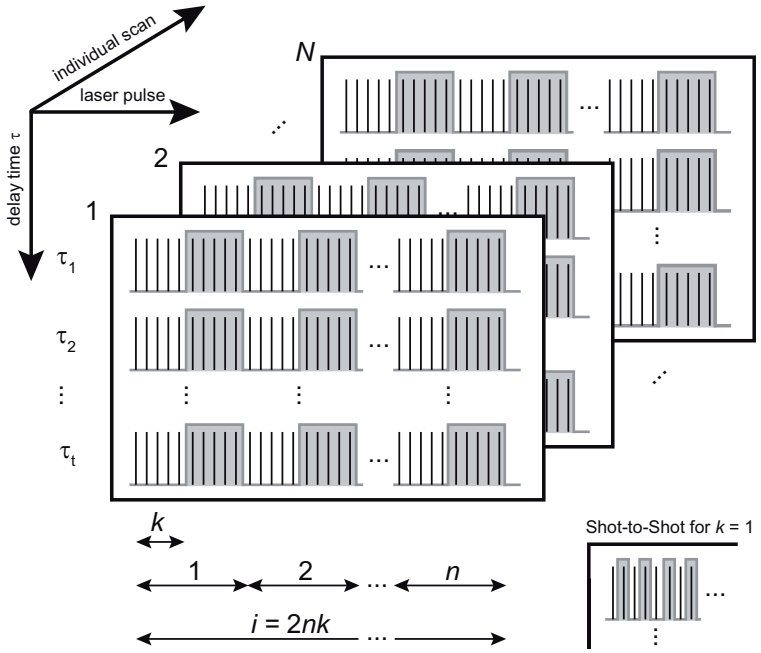

Fig. 1. Typical scheme for measuring and calculating changes in absorbance Δa. For k probe pulses averaged on the detector the chopper either blocks or transmits k corresponding pump pulses (state of the pump chopper shown in gray). At a given delay time τ the change in absorbance is averaged over n values of Δa, resulting in an overall number of i recorded pulses. Afterwards a set of N transient maps each one consisting of t delay times τ can be averaged. For $k = 1$ the calculation of Δa is shot-to-shot (inset on lower right).

If the incident probe intensities are equal and do not fluctuate between the two measurements then Eq. (2) and Eq. (3) give the same result; otherwise an error is introduced. Thus the evaluation with Eq. (3) works well if the intensities between successive measurements are well correlated. Since this condition is fulfilled on a shot-to-shot basis for 1-kHz laser systems, shot-to-shot detection is advantageous and is nowadays employed in many laboratories by blocking every second pump pulse. However, finite data readout times of the detector and the maximum speed of the pump-beam chopper have so far limited this approach to lasers with repetition rates of a few kHz.

For high repetition rates ($\geq$ 100 kHz) one typically averages I_p and I_u each over k probe pulses on the detector. The change in absorbance is calculated for two subsequent averaged sequences of k probe pulses with the corresponding pump pulses blocked or unblocked (Fig. 1, state of the chopper highlighted in gray). For one delay time τ the change in absorbance is averaged n times. The number of detected pulses is $i = 2nk$ for each τ (Fig. 1). The averaging of the change in absorbance is repeated for t time delays τ constructing a transient map. The signal-to-noise ratio can further be improved by averaging over N individual transient maps measured successively.

It was shown by Polack et al. that a 400-nm pump beam can be chopped by a mechanical chopper synchronized to a 100-kHz laser [2, 3]. A midinfrared probe and reference beam were measured spectrally integrated with 100 kHz on two HgCdTe detectors. Using a lock-in amplifier the 50-kHz pump-beam modulation was filtered from the difference in the transmitted probe and the reference beam. The change in absorbance sent from the lock-in amplifier was

#209006 - $15.00 USD Received 26 Mar 2014; revised 9 May 2014; accepted 19 May 2014; published 3 Jul 2014

averaged for 30,000 pulses. To our knowledge, spectrally resolved broadband shot-to-shot detection has not been reported for high-repetition-rate lasers > 20 kHz [4]. Here we demonstrate shot-to-shot broadband detection of transient absorption spectra by combining synchronized mechanical chopping of a 100-kHz laser and a commercially available fast CCD line camera.

2. Experimental setup

For a shot-to-shot calculation of the change in absorbance Δa the pump beam has to be blocked for every second pulse. In principle, this task can be approached in various ways. Acousto–optic modulators (AOMs) can be used to diffract into a slightly different direction every second pulse up to several hundred kHz repetition rates. The diffracted beam can then be used as the modulated pump beam. However, the dispersion added to the pulses in AOM crystals stretches the pulse length significantly. This issue can be overcome if acousto–optic programmable dispersive filters (AOPDFs) are used as the pulse can be compressed simultaneously [5]. AOMs and AOPDFs are restricted to certain wavelength ranges depending on the crystals used. Another disadvantage is their relatively high cost.

For few-kHz lasers the use of commercially available mechanical chopper wheels is well established [6–8]. They can be triggered externally by the laser trigger. In that case, jitter of the rotation is so small that it does not affect correct chopping. With high motor turning speeds and an adequate number of slots in the chopping wheel chopping rates can be increased up to over 100 kHz. Pulse energy and pulse duration remain unaltered facilitating nonlinear processes for frequency conversion such as noncollinear optical parametric amplification (NOPA) at high repetition rates [9]. Appropriate laser synchronization is critical, however.

We developed a high-speed mechanical chopper based on a brushless DC motor (Nanotec DB42M02) in combination with a programmable motion controller (Trinamic TMCM-171). The chopper unit is equipped with a commercially available chopper wheel (300D445, Scitec instruments) with 445 slots of 340 μm in diameter to block every second pump pulse in our transient absorption setup operated with a 100-kHz laser (Fig. 2). The required turning speed of about 112.5 rotations per second (rps) is set in the motion controller of the motor and controlled by a speed sensor at the rotation axis. Compared to few-kHz repetition rates, at a repetition rate of 100 kHz the jitter of the axis rotation gets critical, i.e., pulses might either be blocked or transmitted wrongly if laser and chopper are not perfectly synchronized. Since the chopper is a mechanically rotating disk, its moment of inertia makes rapid adjustments of the chopper frequency challenging. Therefore, we synchronized the laser to the rotation frequency of the chopper rather than vice versa. A home-built light barrier at the chopper wheel generates a 50-kHz trigger representing the passage of slots in the chopper wheel. The 50-kHz trigger is doubled in frequency by adding a copy of itself with an adjustable delay resulting in the 100-kHz master trigger. The 38-MHz trigger output provided by the control unit of the Ti:Sa oscillator (Coherent Mira 900, 76 MHz) is electronically reduced to 100 kHz with a double “flip-flop” circuit, picking each first pulse coinciding with the master trigger (“Synchronization” in Fig. 2, a connectivity diagram is given in the Appendix). Thus it is ensured that only oscillator pulses are injected by the cavity dumper of the amplifier (Coherent RegA 9000) which will thereafter pass a slot of the chopper wheel or will be blocked, i.e., pump pulses are neither wrongly blocked nor wrongly transmitted by the chopper wheel. The jitter of the chopper was determined to be below 1 μs. Anyhow, the jitter is not critical for the amplification because a Q-switch prevents lasing of the continuously pumped Ti:Sa crystal as long as no trigger pulse is sent from the chopper, i.e., as long as no oscillator pulse is injected into the amplifier cavity.

The amplified pulses have a typical pulse energy of 3 μJ and a pulse length of about 170 fs at a central wavelength around 800 nm. The output of the amplifier is split into two parts. One fraction ($\approx 30\%$) is sent through a telescope ($f_1 = 100$ mm, $f_2 = 125$ mm) with the chopper

#209006 - $15.00 USD Received 26 Mar 2014; revised 9 May 2014; accepted 19 May 2014; published 3 Jul 2014

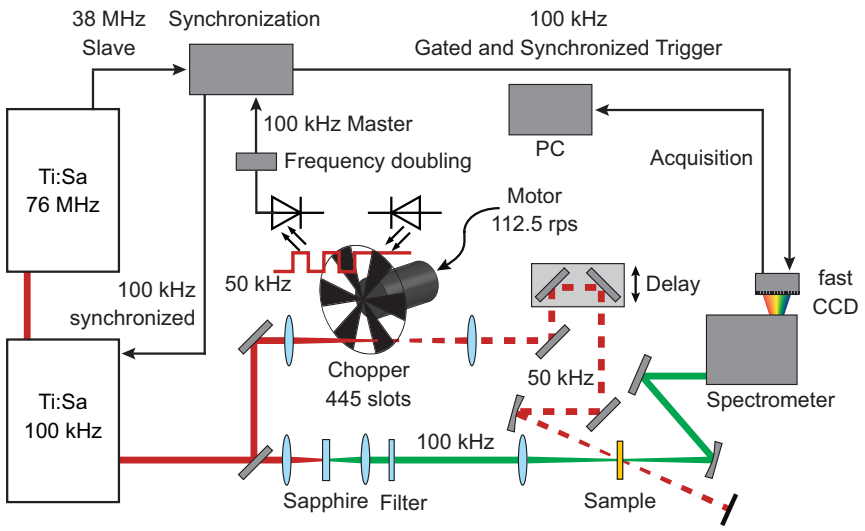

Fig. 2. Experimental setup for 100-kHz shot-to-shot transient absorption spectroscopy. A light barrier attached to the chopper produces a 100-kHz master trigger which is synchronized to the trigger signal output of the oscillator. The amplifier is triggered by the synchronized trigger to ensure that only pulses matching the chopper wheel rotation are amplified. A detailed explanation is given in the text. A connectivity diagram of the synchronization box can be found in the Appendix.

wheel placed in its focus. After passing the chopper unit, the beam travels along a motorized linear delay stage (Newport M-IMS600LM) and is focused with a spherical mirror ($f = 200$ mm) into the 200-μm path-length flow-cell sample cuvette (beam diameter 210 μm). The major part of the amplifier output is focused in a 1-mm sapphire plate ($f = 125$ mm) to produce a white-light supercontinuum probe beam. This whitelight continuum is recollimated and the 800-nm fundamental part is reflected with a "hot mirror" (Thorlabs FM01) transmitting the visible spectrum below 720 nm. The probe beam is focussed with a lens ($f = 150$ mm) into the sample cell (beam diameter 160 μm) and overlapped with the 800-nm pump beam. Both beams are horizontally polarized. The sample is circulated with a micro annular gear pump (mzr-4605, hnp Mikrosysteme GmbH). The synchronized 100-kHz trigger signal is electronically gated to trigger the acquisition of i pulses with a fast CCD line camera (e2v AViiVA EM4, 1024 pixels, pixel size 14×28 μm) attached to a spectrometer (SpectraPro500, Acton Research Corporation, 150 g/mm grating blazed at 500 nm). Thus we measure the spectrum of each single probe pulse. As the pump beam is modulated with half the repetition rate, the change in absorbance Δa is calculated from the intensities for pairs of successive probe pulses according to Fig. 1 (inset) and Eq. (3) for the whole recorded spectrum. The difference spectrum for each τ is averaged for n pulse pairs. After acquisition of the averaged difference spectrum the delay stage is moved to the position corresponding to the next delay time τ. After scanning t delay times, the scan is repeated N times, averaging N difference spectra for each τ (Fig. 1).

As described in the next section, a transient absorption experiment is typically conducted with $k = 1$, $n = 500$, $t = 200$, and $N = 10$. For this set of acquisition parameters, the total measurement time is about 30 min, i.e., 3 min for one single transient map which is a measurement speedup by about a factor of > 3 compared to our 1-kHz transient absorption setup [6]. For $N = 1$ ($i = 2 \times 10^5$) the overall probe pulse acquisition within our data acquisition program takes about 80 s. The 200 movements of the linear delay stage take about 90 s. In sum, the cal-

#209006 - $15.00 USD Received 26 Mar 2014; revised 9 May 2014; accepted 19 May 2014; published 3 Jul 2014

culation and averaging of the change in absorbance in the measurement computer takes about 10 s for one set of delay times. With a delay stage allowing a fast-scan measurement [10] and parallel data acquisition allowing the delay stage to move continuously while taking data on the fly [11, 12] the overall measurement time could be further reduced.

3. Transient absorption data

As a benchmark we conducted transient absorption spectroscopy on the laser dye IR 140 [13–15] dissolved in ethanol. When excited with pulses around 800 nm, IR 140 shows excited-state absorption (ESA) between 500 and 650 nm [14] whose maximum ($\lambda_{\max} = 565$ nm) is attributed to S_1–S_n absorption [13]. The ESA decay is reported to be a biexponential process with a fast time constant of 1.96 ps and a slow time constant of greater than 100 ps [14]. For a monoexponential data analysis a decay time constant of 0.5 ns was obtained [13].

In our experiment the pulse energy of the pump beam was adjusted to 186 nJ, the probe beam had a pulse energy of about 20 nJ. Due to a small remaining transmission of the fundamental beam through the hot mirror, a larger probe pulse energy was detected as the roughly 8 nJ expected from the maximum spectral density of whitelight generated in a sapphire crystal [16]. Each recorded transient map consists of $t = 200$ delay time steps, split into 100 time steps of 50 fs from -2 ps to 3 ps and 100 logarithmically increasing time steps from 3 ps to 1.2 ns. The data was averaged for $k = 1$, $n = 500$, $t = 200$, and $N = 10$.

The result of the dynamics in a wavelength range from about 435 to 640 nm is shown in Fig. 3(a) in a delay time interval τ ranging from -0.25 to 1000 ps. A global lifetime analysis [17] was done by fitting the data with the open-source graphical interface Glotaran [18] working with the statistical fitting package TIMP [19]. For a two-exponential model a rising lifetime of $\tau_1 = 169$ fs reflecting the pump pulse length and a decaying lifetime of $\tau_2 = 620$ ps were obtained. Considering that in Ref. [14] data was fitted for single wavelengths only and in a limited temporal window of up to 300 ps these results are consistent with the literature [13, 14].

Figure 3(b) shows difference spectra for various delay times. The temporal evolution of the change in absorbance can be seen in Fig. 3(c) for a selection of probe wavelengths at 500, 540, and 565 nm. The recorded data (crosses) and the biexponential global fit (dashed lines) agree very well, demonstrating high signal-to-noise ratio and thus the feasibility of significantly reduced total measurement time using 100-kHz shot-to-shot detection.

In general, for all high-repetition-rate pump–probe experiments—regardless of the detection technique—the exchange of the excitation volume has to be considered for every studied molecular system [4]. Uncomplete sample exchange might lead to an offset signal for decay lifetimes larger than the repetition rate's periodic time (in our case $\tau \geq 10$ µs). If dynamics of chemical reactions are studied, the excitation energy has to be kept low, which is an intrinsic advantage of high-repetition-rate lasers, so that distortion of the measured signal by photoproduct absorption is minimized.

4. Noise-level analysis

In spectroscopic measurements several different noise sources can contribute. We consider electronic noise of the camera, shot noise, and laser fluctuation. Their effects on the error of Δa are calculated by error propagation and summarized in Table 1.

The overall electronic noise contribution of the camera, e.g., basically read-out noise, is 7.7 LSB (least significant bit), corresponding to 7.7 counts. Let us consider an average count rate at 70% of the full dynamic range of the 12-bit ADC, i.e., 0.7×2^{12} counts $= 2870$ counts. This leads to a relative error of 2.68×10^{-3}. The shot noise due to Poissonian statistics is the square root of the number N_{Ph} of incident photons on the detector. For an average detector quantum efficieny of 0.75 in the wavelength range from 430 to 700 nm and again an

#209006 - $15.00 USD Received 26 Mar 2014; revised 9 May 2014; accepted 19 May 2014; published 3 Jul 2014

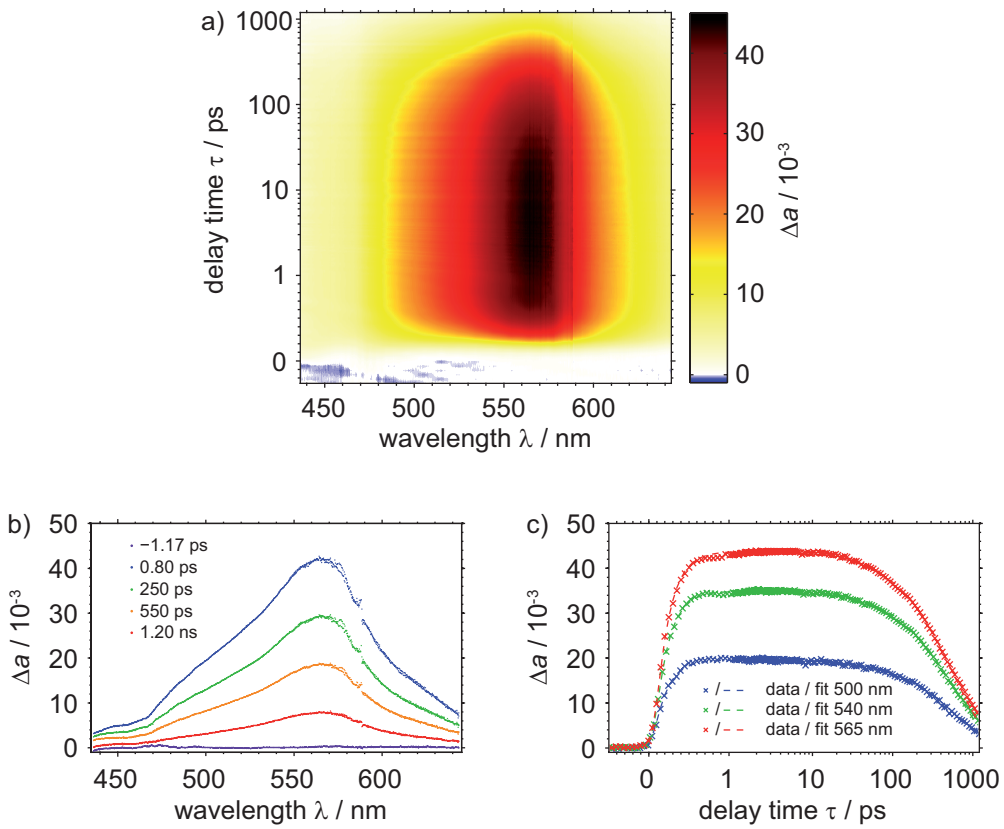

Fig. 3. Transient absorption data of IR 140 in ethanol measured shot-to-shot at 100-kHz repetition rate. a) The transient map was recorded with excitation at 800 nm and a sapphire whitelight probe continuum. Data was averaged for $k = 1$, $n = 500$, $t = 200$, and $N = 10$. Note that the delay time axis changes from linear to logarithmic scaling for $\tau > 1$ ps. b) The ESA can be seen in the difference spectra for various delay times. The spike in all difference spectra around 590 nm originates from a dip in the whitelight probe spectrum. c) The dynamics of the ESA are shown by transients for three different wavelengths. The dashed lines indicate the results of a global lifetime analysis.

Table 1. Noise contributions and error for the calculated change in absorbance Δa.

	noise contribution		
	electronic noise	shot noise	laser fluctuations[a]
value	$I_0 = 2870$ counts	$N_{\mathrm{Ph}} = 2.22 \times 10^5$	$I_0 = 2870$ counts
error	7.7 LSB[b] $\hat{=}$ 7.7 counts	$\sqrt{N_{\mathrm{Ph}}} = 471$	$\Delta I_0 = 35$ counts
relative error	2.68×10^{-3}	$1/\sqrt{N_{\mathrm{Ph}}} = 2.12 \times 10^{-3}$	1.22×10^{-2}
error[c] of Δa	1.65×10^{-3}	1.30×10^{-3}	7.49×10^{-3}

[a]intensity value for single pulses at 537.4 nm; [b]least significant bit; [c]after error propagation

exploitation of 70% of the pixels' wells (full well capacity $= 2.38 \times 10^5$ electrons per pixel), $N_{\mathrm{Ph}} = (0.7/0.75) \times 2.38 \times 10^5 = 2.22 \times 10^5$. Therefore, the relative error due to shot noise (shot-noise limit) is $1/\sqrt{N_{\mathrm{Ph}}} = 2.12 \times 10^{-3}$. To estimate the laser fluctuations, we recorded subsequent probe pulse intensities I_0 on one pixel of the fast CCD line camera at 537.4 nm. The

#209006 - $15.00 USD Received 26 Mar 2014; revised 9 May 2014; accepted 19 May 2014; published 3 Jul 2014

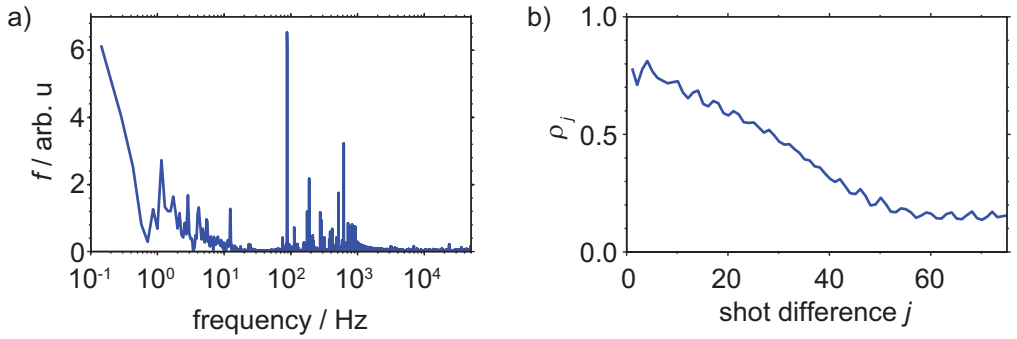

Fig. 4. Noise and correlation analysis at 537.4 nm. a) The Fourier transform f of $i = 7 \times 10^5$ intensities $I_{0,m}$ on one pixel for subsequent probe pulses reveals dominant low-frequency contributions up to roughly 1 kHz. b) The high correlation between probe pulses calculated for $i = 2^{15}$ decreases for greater temporal spacing.

measured intensity values contain errors from the other noise contributions as well. However, as can be seen from Table 1, the different noise contributions are significantly smaller than the error for the measured intensities, i.e., the intensity fluctuations are a direct measure of the laser fluctuations. For an average count number of 2870, the absolute error of the probe pulse intensity is about 35 counts, i.e., the relative error is 1.22×10^{-2}. Assuming uncorrelated intensity values I and I_0, error propagation of the Δa calculation according to Eq. (3) leads to the absolute Δa errors shown in the last row of Table 1. The laser fluctuations clearly dominate over the other noise contributions, which has been shown earlier for 1-kHz lasers [20]. For the 12-bit digitizer, the maximal detection sensitivity for Δa (resulting from a pump-induced change in the probe intensity count rate of 1 bit) at 70% of saturation is $\lg[0.7 \times 2^{12}/(0.7 \times 2^{12} - 1)] = 1.51 \times 10^{-4}$ and hence below the noise contributions. Considering the results from Table 1, it becomes clear that reducing the influence from laser fluctuations has the strongest impact among the various noise contributions on the overall signal-to-noise level. Thus the order of the averaging and recording procedure (Fig.1) becomes relevant and shot-to-shot detection advantageous.

To test the effect of the reduced shot-to-shot measurement time on the signal-to-noise ratio compared to an acquisition method with $k \gg 1$, we performed a noise-level analysis. Shot-to-shot detection is advantageous for ∼1-kHz-repetition-rate lasers because subsequent laser pulses are strongly correlated. For a shot difference greater than one laser pulse the correlation rapidly decreases [21]. In order to find out whether this correlation also holds for whitelight supercontinuum probe pulses at 100 kHz, we recorded i intensity values I_0 on one pixel of the fast CCD line camera corresponding to a wavelength of $\lambda = 537.4$ nm. The noise-frequency contributions f for a series of i pulses are given by the absolute value of the Fourier transform $\mathcal{F}$ of the intensities $I_{0,m}$ with $m = 1, 2, ..., i$:

$$f = |\mathcal{F}\{I_{0,1}, I_{0,2}, ..., I_{0,i}\}|. \tag{4}$$

In this measurement the chopper is only used for generating the master trigger, but neither the pump pulses nor the sample cuvette are used.

It has previously been shown that low-frequency contributions dominate the noise characteristics of few-kHz lasers [20, 22]. Also for our 100-kHz laser the noise is dominated by low-frequency contributions ranging up to roughly 1 kHz (Fig. 4(a)). Therefore calculation of the change in absorbance by averaging I_p and I_u for $k \gg 1$ probe pulses is unfavorable, and shot-to-shot data acquisition ($k = 1$) should be advantageous also for high-repetition-rate lasers.

#209006 - $15.00 USD Received 26 Mar 2014; revised 9 May 2014; accepted 19 May 2014; published 3 Jul 2014

We also calculated the statistic autocorrelation ρ_j for a series of i probe pulses,

$$\rho_j = \frac{1}{\sigma^2 i} \sum_{m=1}^{i-j} [(I_{0,m} - \mu)(I_{0,\,m+j} - \mu)], \tag{5}$$

with $j = 0, 1, 2, ..., i-1$, where σ^2 is the variance and μ is the mean value of the intensities $I_{0,m}$. The statistic autocorrelation is shown in Fig. 4(b) for a wavelength of 537.4 nm and a sequence of $i = 2^{15}$ probe pulses. It can clearly be seen that with the employed 100-kHz laser successive pulses are strongly correlated. The correlation drops within ≈ 50 pulses. This directly shows that measurement with $k = 1$ is superior to $k \gg 1$ and therefore, the estimated error of Δa from Table 1 can be reduced.

To quantify the advantage of shot-to-shot detection we calculated Δa via Eq. (3) for one CCD pixel but without any pump beam present. Ideally this should lead to $\Delta a = 0$, with the remaining signal indicating the noise floor. We compare two different situations: the "conventional" measurement scheme by emulating a CCD camera with 1-ms readout time via averaging over $k = 100$ shots (Fig. 5, blue); and the new shot-to-shot measurement scheme using $k = 1$ (Fig. 5, green). As shown above (Table 1), laser noise is the limiting factor in the calculation of Δa and other noise contributions can be neglected for the comparison of different acquisition and averaging schemes. Using just one sequence $n = 1$ for each "timestep" (Fig. 5(a)), the standard deviation σ of Δa is comparable for both scenarios, even though the shot-to-shot technique (green, $\sigma = 2.96 \times 10^{-3}$) uses 100 times fewer pulses than the conventional scheme (blue, $\sigma = 2.34 \times 10^{-3}$). The error of the shot-to-shot detection is about as large as estimated from error propagation in Table 1. Shot-to-shot detection thus has the potential to be 100 times faster than $k \gg 1$ averaging at comparable signal-to-noise ratio.

Comparing the same acquisition time, i.e., the same number ($i = 1000$) of acquired pulses (Fig. 5(b)), the standard deviation for shot-to-shot detection ($k = 1$, $n = 500$, green, $\sigma = 1.2 \times 10^{-4}$) over $t = 200$ delay times is about a factor of 3 smaller than for $k = 100$ ($n = 5$, blue, $\sigma = 4.1 \times 10^{-4}$). Additional improvement on the signal-to-noise ratio could be achieved by even shorter measurement times and more efficient averaging for the given pulse correlation in the fast-scan measurement scheme [10, 11].

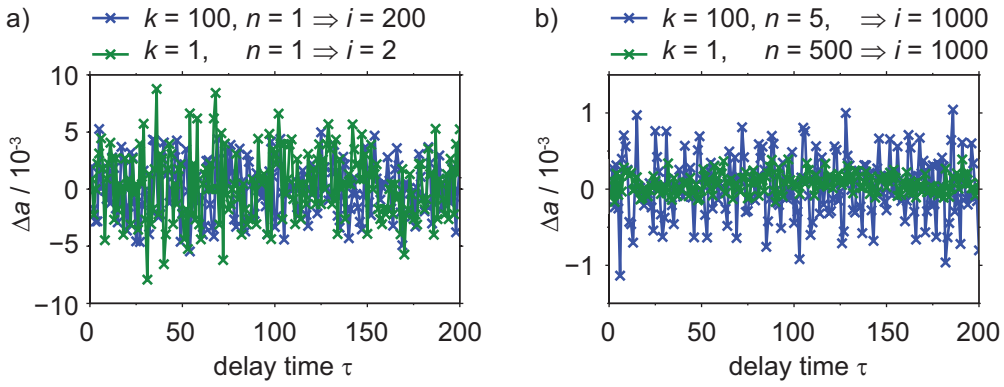

Fig. 5. Comparative noise-level analysis for $k = 100$ and $k = 1$ (shot-to-shot). a) For a single calculation of Δa ($n = 1$) for each delay time τ the noise level is equivalent for ($k = 100$, $i = 200$) and ($k = 1$, $i = 2$). b) For the same number of acquired pulses ($i = 1000$) the noise level is about a factor of 3 smaller for $k = 1$ than for $k = 100$.

#209006 - $15.00 USD Received 26 Mar 2014; revised 9 May 2014; accepted 19 May 2014; published 3 Jul 2014

Even though this comparison does not take into account any error contribution from the pump pulse, it is obvious that averaging over shot-to-shot Δa values results in either significantly reduced total measurement time (Fig. 5(a)) or superior data quality (Fig. 5(b)) for optical pump–probe experiments.

5. Conclusion and outlook

Using a home-built mechanical chopper we were able to modulate the pump beam in an optical pump–probe experiment with half of the laser's repetition rate of 100 kHz. Synchronization was achieved by using the chopper as a master trigger for the laser amplifier. Hence jitter in the chopper rotation frequency is not critical. A fast CCD line camera made it possible to measure the spectrum of every probe pulse at the rate of 100 kHz. We illustrated the capabilities of high-repetition-rate shot-to-shot detection on the transient absorption of IR 140 in ethanol.

The high-repetition scheme considerably decreases the total measurement time required for reaching a particular noise level, potentially by two orders of magnitude when changing from 1 kHz to 100 kHz readout. The maximum speedup may be limited by the reaction time of the linear delay stage, but the potential for measuring quickly decomposing or sensitive samples such as biological complexes is obvious [8]. Another advantage is that kinetic processes like aggregate formation or kinetically oscillating reactions could be studied.

With further improvement of fast CCD devices shot-to-shot data acquisition might be possible for repetition rates higher than 100 kHz, e.g., 250 kHz, which is also common for high-repetition-rate amplified lasers. Adapting the scheme for data acquisition in coherent multidimensional spectroscopy should be straightforward.

Appendix

Figure 6 shows the connectivity diagram of the "Synchronization" electronics from Fig. 2 used to synchronize chopper, laser, and CCD acquisition.

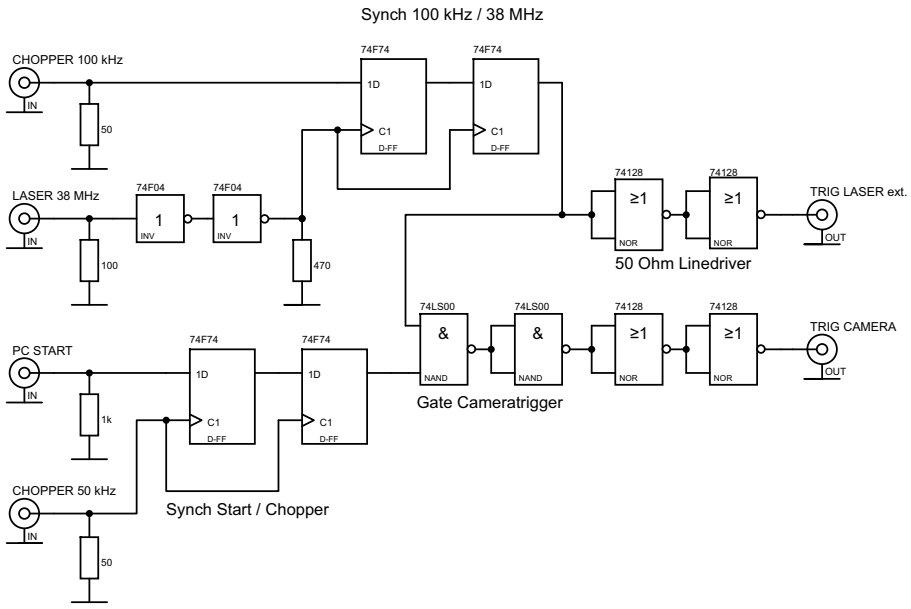

Fig. 6. Connectivity diagram of the synchronization electronics.

#209006 - $15.00 USD Received 26 Mar 2014; revised 9 May 2014; accepted 19 May 2014; published 3 Jul 2014

Acknowledgments

We are grateful to the Deutsche Forschungsgemeinschaft (DFG) for financial support within the Research Unit "Light-Induced Dynamics in Molecular Aggregates" (FOR 1809). We thank Patrick Nuernberger as well as the group of Antigoni Alexandrou and Sergey P. Laptenok for providing incentives on the high-speed mechanical chopper and Johannes Buback for his help with the CCD camera. FK further acknowledges financial support from the "Fonds der Chemischen Industrie". This publication was funded by the Deutsche Forschungsgemeinschaft (DFG) and the University of Würzburg in the funding program Open Access Publishing.

#209006 - $15.00 USD Received 26 Mar 2014; revised 9 May 2014; accepted 19 May 2014; published 3 Jul 2014